Fast non-destructive assessment of heavy metal presence by ATR–FTIR analysis of crayfish exoskeleton

Maria Grazia Volpe, Daniela Ghia, Omid Safari & Marina Paolucci

Environmental Science and Pollution Research

ISSN 0944-1344

Environ Sci Pollut Res
DOI 10.1007/s11356-020-08405-z

Springer

Environmental Science and Pollution Research
https://doi.org/10.1007/s11356-020-08405-z

RESEARCH ARTICLE

Fast non-destructive assessment of heavy metal presence by ATR–FTIR analysis of crayfish exoskeleton

Maria Grazia Volpe[1] · Daniela Ghia[2] · Omid Safari[3] · Marina Paolucci[1,4]

Received: 1 July 2019 / Accepted: 12 March 2020

Abstract

Freshwater crayfish are bioindicators of environmental pollution, often used for the assessment of heavy metal (HM) presence in the tissues, a time-consuming and expensive task. In this study, we propose the use of the vibrational spectroscopy to detect in a fast, non-destructive and sensitive way the presence of HM in the cephalothorax exoskeleton of the freshwater crayfish. Incorporation of HM into the cephalothorax exoskeleton was investigated under controlled laboratory conditions. In particular, the cephalothorax exoskeleton of five crayfish species (*Astacus leptodactylus*, *Procambarus clarkii*, *Austropotamobius pallipes*, *Faxonius limosus*, and *Pacifastacus leniusculus*) was analyzed by attenuated total reflection–Fourier transformed infrared (ATR–FTIR) spectroscopy in the presence or absence of cadmium (Cd), chromium (Cr), lead (Pb), nickel (Ni), and zinc (Zn) up to 4 weeks at various concentrations (0.01, 0.1, 1, 10, ppm). The ATR–FTIR profile of the crayfish cephalothorax exoskeleton was compatible with the presence of amorphous calcium carbonate, chitin, and proteins. The incubation with the HM revealed two main modifications: the shift of the peak from 859 to 872 cm^{-1} and the appearance of a peak at 712 cm^{-1}. Both are ascribable to the HM interaction with calcium carbonate. The absorbance of both peaks increased along with the time of incubation, and the HM concentration. We conclude that ATR–FTIR analysis can be a useful, quick, and cost-sensitive tool to detect HM presence in the crayfish cephalothorax exoskeleton. However, it has to be regarded as a non-specific analytical technique for assessing HM contamination, since it is unable to discriminate between different HM.

Keywords Crayfish · Cephalothorax exoskeleton · Heavy metals · ATR–FTIR · Bioassays

Introduction

Heavy metals (HM) are natural components of the earth's crust. They can be divided into essentials which are, as the name suggests, necessary to support biological functions, and non-essentials that are toxic even at low concentrations (Ali et al. 2019). Non-essential metals bind to cellular components, such as proteins and nucleic acids, damaging the performance of vital functions (Igiri et al. 2018). They can damage the nervous system, cause renal dysfunction, bone degeneration, and liver and blood damage, and cause reproductive dysfunctions in living organisms (Assi et al. 2016). However, even the essential metals, although crucial for maintaining a proper metabolism, in higher concentrations are toxic (Jaishankar et al. 2014; Prashanth et al. 2015). HM such as cadmium (Cd), chromium (Cr), lead (Pb), nickel (Ni), and zinc (Zn) are among the most common pollutants found in industrial effluents (Rajaganapathy et al. 2011). HM pollution caused by human waste disposed in water courses is a devastating phenomenon of global proportions. The impact on ecosystem wildlife is severe. Maintaining suitable freshwater quality is essential for both aquatic and terrestrial life, and monitoring of metal concentration in freshwater based solely on toxicity

Responsible editor: Philippe Garrigues

✉ Marina Paolucci
paolucci@unisannio.it

[1] Institute of Food Sciences –National Research Council (ISA-CNR), Via Roma 64, 83100 Avellino, Italy

[2] Department of Earth and Environmental Sciences, University of Pavia, Via Taramelli 24, 27100 Pavia, Italy

[3] Department of Fishery, Faculty of Natural Resources and Environment, Ferdowsi University of Mashhad, Mashhad, Iran

[4] Department of Science and Technologies, University of Sannio, Via Port'Arsa, 11, 82100 Benevento, Italy

Published online: 07 April 2020

studies of dissolved contaminants may not be indicative of the real accumulation in the tissues of living organisms. Macroinvertebrates, such as crayfish, are frequently suggested as bioindicators for monitoring water conditions in polluted areas (Alikhan et al. 1990; Zhou et al. 2008; Kuklina et al. 2013; Pallottini et al. 2015), since HM accumulates in their tissues, especially through the food chain (Bruno et al. 2006; Kouba et al. 2010).

One way to evaluate the contamination of the water body is to calculate the quantity of selected elements accumulated in the tissues of target organisms. Indeed, tissue analysis could provide useful information both on the level of pollution and the bioavailability of specific metals (Suárez–Serrano et al. 2010; Goretti et al. 2016). Furthermore, some crayfish are considered to be highly resistant to environmental metal contamination (Del Ramo et al. 1987; Kouba et al. 2010), which makes them suitable bioindicators. The accumulation of metals in their tissues is dose- and time-dependent, and therefore may be reflective of the levels of metals in the environment (Alcorlo et al. 2006; Kuklina et al. 2014). Earlier studies have indicated that the crayfish exoskeleton is a highly efficient natural material effective absorbent for the removal of Pb, Cd, Zn, and copper (Cu) from aqueous solutions (Zheng et al. 2010). The exoskeleton of crayfish consists of an organic matrix composed mainly of chitin and proteins forming a network of fibrils closely associated with amorphous calcium carbonate, the predominant mineral (Stein and Murphy 1976; Huner et al. 1990; Shechter et al. 2008). It contains 40% amorphous calcium carbonate, 30% protein, and 30% chitin (Giraud-Guille et al. 2004). The unique physical and chemical properties of crayfish exoskeleton are likely due to its highly ordered structure, leading to certain characteristics that most inorganic crystals do not possess (Wang et al. 2016). The mechanism of HM uptake onto crayfish exoskeleton implies physical adsorption, chemical precipitation, chemical chelation, and ion exchange (Wang et al. 2016). The unique physical and chemical properties of crayfish exoskeleton induced us to exploit its characteristics as a bioindicator of the conditions of HM water pollution. Thus, in this study, we analyzed the absorption capacities of the crayfish exoskeleton exposed to different concentrations of Cd, Cr, Ni, Pb, and Zn, by attenuated total reflection–Fourier transformed infrared (ATR–FTIR) spectroscopy. Transmission spectroscopy is a common method for identifying molecular structure, and chemical bonding of organic and inorganic chemicals. Environmental applications of ATR–FTIR focused on HM identification are mainly dedicated to the investigation of the chemical mechanisms underlying the binding between the HM with both artificial and natural materials (Simonescu 2012). In this study, we focused on the possibility offered by the ATR–FTIR to make component analysis of the exoskeleton of crayfish species (*Astacus leptodactylus*, *Procambarus clarkii*, *Austropotamobius pallipes*, *Faxonius limosus*, *Pacifastacus leniusculus*). Crayfish exoskeleton is a highly efficient natural absorbent of heavy metals, whose absorption capacity is higher than some natural absorbents such as chitin and chitosan and synthetic absorbents usually employed to remove heavy metals from contaminated waste waters (Zheng et al. 2010; Wang et al. 2016). Continuous exposure of crayfish to a low concentration of heavy metals, mainly through the food chain, may result in bioaccumulation (Suárez–Serrano et al. 2010; Goretti et al. 2016). Since the crayfish exoskeleton binding HM shows a distinctive ATR–FTIR profile, the exoskeleton has the potential to become an excellent tool for monitoring water pollution. Thus, we propose the feasibility of ATR–FTIR analysis as an analytical method to detect in a green way heavy metal environmental contamination and to carry on the simultaneous analysis of multiple components of the same sample in a single instrumental measurement without environmental side effects. Thus, the primary objective of this study was to analyze by ATR–FTIR interactions of Cd, Cr, Pb, Ni, and Zn dissolved in water, with the crayfish cephalothorax exoskeleton, to establish a model that could be employed for rapid and cost-effective assessment of the HM presence in the aquatic environment.

Materials and methods

Animals

Only adult crayfish in intermolt were employed. Only the cephalothorax exoskeleton was collected, thoroughly washed, and dried in the air. Since accumulation of HM in crayfish is not influenced by sex (Anderson and Brower 1978), in this study, we used both sexes. *A. leptodactylus* were obtained from the Shahid Yaghoobi reservoir (35° 9′ 36″ N, 59°24′ 18″ E, Khorasan Razavi Province, Iran); *P. clarkii* were purchased from a commercial farm (Ittica Volturno, S.S. 158 Km 26+490¸ Venafro-Roccaraso Road, occhetta al Volturno (IS)); *A. pallipes* were collected in the Stream Pedoca (45° 43′ N, 9° 42′ E) and from the Prabione breeding facility (45° 45′ N, 10° 44′ E); *P. leniusculus* were collected in the Stream Valla (44° 31′ N, 8° 20′ E); *F. limosus* were collected from the River Ticino (45° 37′ N, 8° 39′ E). The crayfish were sacrificed immediately after capture. Considering the protected status of *A. pallipes* species, both at the European and regional

level (Habitats Directive 92/43/EEC, Italian regional law L.R10/2008 Lombardy), we collected and analyzed specimens recently dead for natural causes for this species. Only in the case of *A. leptodactylus*, specimens were kept in laboratory aquaria for several weeks. During the storage period, specimens were fed with formulated diets (composition and manufacturing according to Volpe et al. 2008, 2012).

Adsorption capacities

To carry on the adsorption capacity studies, the cephalothorax exoskeleton was used as a whole and in powder. It was incubated with 0.01, 0.1, 1.0, and 10.0 ppm or mg l^{-1} of Cd, Cr, Pb, Ni, and Zn (Sigma-Aldrich, Saint Louis, USA) in artificial freshwater (Morel and Hering 1993) at pH 7.0 at 20 °C. Since no significant differences were detected in the ATR–FTIR profile of the cephalothorax exoskeleton of the crayfish species (see Table 2), the cephalothorax exoskeleton of *A. leptodactylus* was employed in the following experiments. A total of 0.2 g of powdered cephalothorax exoskeleton was incubated with 20 ml solution of each HM in a test tube, and the tube was placed on a rocking plate for 2 h. The control was represented by the powdered cephalothorax exoskeleton incubated with artificial freshwater without HM. Thereafter, the suspension was centrifuged at 2500 rpm for 10 min. The pellet was dried in an oven and analyzed by ATR–FTIR. In order to mimic a possible environmental exposure to HM, the whole cephalothorax exoskeleton was incubated in a beaker (in a ratio of 1:100, *w*/*v*) with each HM solution at 0.01, 0.1, 1.0, and 10.0 ppm, for 4 weeks, at pH 7.0 at 20 °C. The control was represented by the whole cephalothorax exoskeleton incubated with artificial freshwater without HM. Cephalothorax exoskeleton samples were collected after 1, 2, 3, and 4 weeks, thoroughly washed, and oven dried, then powdered and analyzed by ATR–FTIR. The clearance time was evaluated for 4 weeks after the fourth week of incubation with HM, by incubating the cephalothorax exoskeleton in clean artificial freshwater (in a ratio of 1:100, *w*/*v*). The freshwater was changed every other day. Cephalothorax exoskeleton samples were treated as reported above after the incubation with HM. The experiments were carried out in triplicate.

ATR–FTIR spectra measurements

The cephalothorax exoskeleton was dried and ground into powder in agate mortar. The powder was placed on the germanium piece of the infrared spectrometer and analyzed according to Volpe et al. (2019). The number of crayfish cephalothorax exoskeleton analyzed was the following: *A. leptodactylus* (20), *P. clarkii* (20), *A. pallipes* (10), *P. leniusculus* (10), *F. limosus* (10). Each cephalothorax was analyzed in triplicate. For each experimental group, three samples were analyzed and each sample was analyzed in triplicate.

Statistical analysis

Statistical analysis was performed by the Spectrum AssureID software (trademark of PerkinElmer, Inc. part number 0993 4516 Release E; publication date July 2006; software version 4.x). The description of the analysis is reported in Volpe et al. (2018), except that for cluster analysis, the spectral ranges independently analyzed were the following: (I) 3500–2800, (II) 1680–1350, (III) 1070–990, (IV) 900–650 cm^{-1}. The interclass distance value higher than 3 was indicative that the samples are well separated and hence different (He et al. 2007). The correlation coefficient was calculated by excel statistical functions.

Results

Interpretation of the ATR–FTIR spectra of crayfish cephalothorax exoskeleton

Figure 1 shows the representative ATR–FTIR spectra of the cephalothorax exoskeleton of crayfish *A. leptodactylus*, *P. clarkii*, *A. pallipes*, *F. limosus*, and *P. leniusculus* in the region of 4000–650 cm^{-1}. The assignment of the major bands is shown in Table 1. The assignment of the bands is based on Andersen and Brecevic (1991), Iconomidou et al. (2001), Addadi et al. (2003), Shechter et al. (2008), Movasaghi et al. (2008), and Tao (2013). The statistical analysis carried out with the SIMCA algorithm showed no significant differences among the species. Intergroup distances are reported in Table 2.

HM incubation effects on the ATR–FTIR spectrum of crayfish cephalothorax exoskeleton (powder)

The ATR–FTIR spectrum of the crayfish cephalothorax exoskeleton incubated Cd, Cr, Pb, Ni, and Zn indicates some modifications in the spectral profile. In particular, there was a remarkable shift in the peak at 859 cm^{-1} and the appearance of a peak at 712 cm^{-1} in the presence of the tested concentrations of HM (0.01, 0.1, 1.0, 10.0 ppm) (Fig. 2). The second derivative highlighted the shift of the peak from 859 to 872 cm^{-1}, in the presence of the HM and the appearance of the peak at 712 cm^{-1} (Fig. 2). The statistical analysis carried out on the whole spectrum and in selected spectral ranges revealed a significant difference between the cephalothorax exoskeleton incubated with and without HM in the range 900–650 cm^{-1} (Table 3).

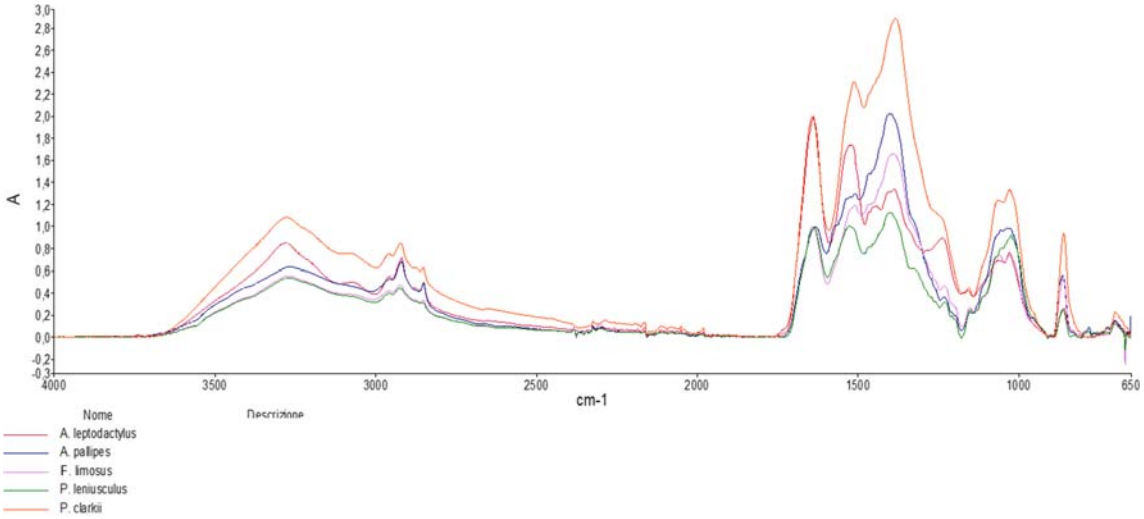

Figure 1 Representative ATR–FTIR spectra of the cephalothorax of crayfish *Astacus leptodactylus*, *Procambarus clarkii*, *Austropotamobius pallipes*, *Faxonius limosus*, and *Pacifastacus leniusculus* in the region of 4000–650 cm^{-1}

HM incubation effects on the ATR–FTIR spectrum of crayfish cephalothorax exoskeleton (whole)

To evaluate the capacity of the whole cephalothorax exoskeleton to bind heavy metals, it was incubated with increasing concentrations (0.01, 0.1, 1.0, 10.0 ppm) of Cd, Cr, Pb, Ni, and Zn up to 4 weeks. Based on the results obtained incubating the cephalothorax exoskeleton powder with Cd, Cr, Pb, Ni, and Zn, the shift of the peak from 859 to 872 cm^{-1} and the appearance of the peak at 712 cm^{-1} were used as markers. The peak shift from 859 to 872 cm^{-1} and the appearance of the peak at 712 cm^{-1} were registered at any of the Cd, Cr, Pb, Ni, and Zn concentrations, at any time of incubation. Both the shift from 859 to 872 cm^{-1} and the appearance of the peak at 712 cm^{-1} are well visible after the second derivative processing (Fig. 3). Cephalothorax exoskeleton samples incubated with Cd, Cr, Pb, Ni, and Zn showed the increase in the absorbance of the peaks at 872 cm^{-1} and 712 cm^{-1}, as well as in the ranges 1560–1350 cm^{-1} and 1070–990 cm^{-1} (Fig. 4). The area of 872 cm^{-1} and 712 cm^{-1} peaks after incubation with increasing concentrations (0.01, 0.1, 1.0, 10.0 ppm) of Pb with the cephalothorax exoskeleton is reported in Fig. 5. The correlation

Table 1 General band assignment of the ATR—FTIR spectra of crayfish carapace in the 4000–650 cm^{-1} spectral range according to the literature (Andersen and Brecevic 1991; Iconomidou et al. 2001; Shechter et al. 2008; Addadi et al. 2003; Movasaghi et al. 2008; Tao 2013)

Spectral ranges (cm^{-1})	Peak Wavenumber (cm^{-1})					
	A. leptodactylus	*P. clarkii*	*A. pallipes*	*F. limosus*	*P. leniusculus*	General assignment
3500–2800	3279	3275	3268	3275	3270	O-H stretching symmetric
	2959	2959	2957	2959	2958	C-H stretching
	2920	2922	2920	2925	2925	C-H stretching
	2851	2853	2851	2853	2853	C-H stretching
1680–1600	1638	1639	1634	1639	1635	Amide I
1560–1470	1518	1509	1507	1509	1526	Amide II
1440–1350	1387	1383	1404	1393	1403	Asymmetrical C-O stretching mode
1070–990	1028	1028	1034	1024	1023	Symmetrical C-O stretching
900–820	859	859	862	861	862	CO_3 out-of-plane deformation
730–660	700	699	698	699	700	OCO bending, in-plane deformation mode

Table 2 The values of the intergroup distances among carapace ATR–FTIR spectra of different species of crayfish. Values higher than 3 are statistically significant

Species	*P. clarkii*	*A. pallipes*	*F. limosus*	*P. leniusculus*
A. leptodactylus	1.59	1.81	1.75	1.86
P. clarkii		1.89	2.24	1.86
A. pallipes			2.52	2.80
F. limosus				1.60

Table 3 The values of the distances between the control carapace (omitted) and the carapaces incubated with cadmium (Cd), chromium (Cr), nickel (Ni), lead (Pb), and zinc (Zn). Values are reported in the all spectral range (4000–650 cm^{-1}) and in selected spectral ranges

Spectral range (cm^{-1})	Cadmium	Zinc	Chromium	Lead	Nickel
4000–650	5.71	9.72	6.99	9.85	7.68
3500–2800	2.40	1.81	1.76	2.71	2.31
1680–1350	1.58	2.51	2.03	1.64	1.97
1070–990	2.19	1.51	2.65	2.06	1.49
900–650	60.01	67.22	65.94	65.32	68.49

Statistical analysis was performed by the Spectrum AssureID software using the SIMCA algorithm ($n = 12$). Values higher than 3 are statistically significant

coefficient r is reported in Fig. 5. After 4 weeks of clearance, no back shift of the peak from 872 to 859 cm^{-1} or disappearance of the 712 cm^{-1} peak occurred. The area of the peaks and the correlation coefficient were calculated. Although the absorbance decreased during the clearance time (Fig. 6), there was no correlation between the peak area and the clearance time for any concentration of HM used (data not shown).

Discussion

The purpose of this study was to investigate the usefulness of ATR–FTIR as a fast way to detect environmental pollution of HM. To achieve this, the crayfish cephalothorax exoskeleton was exposed to different concentrations of Cd, Cr, Pb, Ni, and Zn, and the ATR–FTIR profile recorded to find reliable markers that could be employed as a quick and cost-effective tool for environmental contamination analysis. We analyzed the cephalothorax exoskeleton of five crayfish species, *A. leptodactylus*, *P. clarkii*, *A. pallipes*, *F. limosus*, and *P. leniusculus*. The ATR–FTIR analysis of the cephalothorax exoskeleton of crayfish carried out in this study agrees with its organization, consisting of frameworks of chitin associated with proteins and amorphous calcium carbonate intimately associated to the protein fibrils (Sugawara et al. 2006). Indeed, the ATR–FTIR profile revealed functional groups typical of proteins, chitin, and amorphous calcium carbonate (ACC). The ATR–FTIR profile of the cephalothorax exoskeleton was characterized by a broad band between 1600 and 1200 cm^{-1}, characteristic of ACC (Andersen and Brecevic 1991), but also encompassing the absorbance bands typical of amide I, amide II, and amide III (Iconomidou et al. 2001). In some cephalothorax exoskeleton, the peaks of amides I and II are covered by the broad peak of calcium carbonate, while in others was visible. This is in agreement with Wang et al. (2016), reporting the FTIR spectrum of crayfish exoskeleton after partial decalcification. The broad peak between 1600 and 1300 cm^{-1} visible when the exoskeleton is fully calcified changes shape revealing the amide I and amide II peaks according to the decalcification degree. Thus, according to our results, the variations in the cephalothorax exoskeleton composition may be due to different degrees of calcification during the intermolt phase and related to the environment (water hardness). The variations in the ATR–FTIR profile among the crayfish species analyzed, albeit not significant, are likely to be due to variations in the calcium carbonate content, as a consequence of the continuous transfer of the calcium carbonate from the surrounding water to the exoskeleton (Shechter et al. 2008). Proximate composition of the exoskeleton may vary with size, age, and molt stage (Stein and Murphy 1976). Moreover, variations in crayfish exoskeleton mineralization have been observed in different geographic areas, and a lower level of mineralization has been observed in farmed animals with respect to the wild ones (Jussila 1997; Jussila et al. 1995). In this study, we have analyzed only adult specimens in intermolt period, and although the ATR–FTIR profile shows some differences among species, these are not statistically significant.

In the ATR–FTIR spectrum of the cephalothorax exoskeleton incubated with HM, the in-plane bending of carbonate at 712 cm^{-1} appears. The peak at 712 cm^{-1} is typical of aragonite and calcite, the crystalline polymorphs of calcium carbonate, but not of the ACC (Andersen and Brecevic 1991). The incubation with HM caused the appearance of the 712 cm^{-1} peak. This could be attributed to

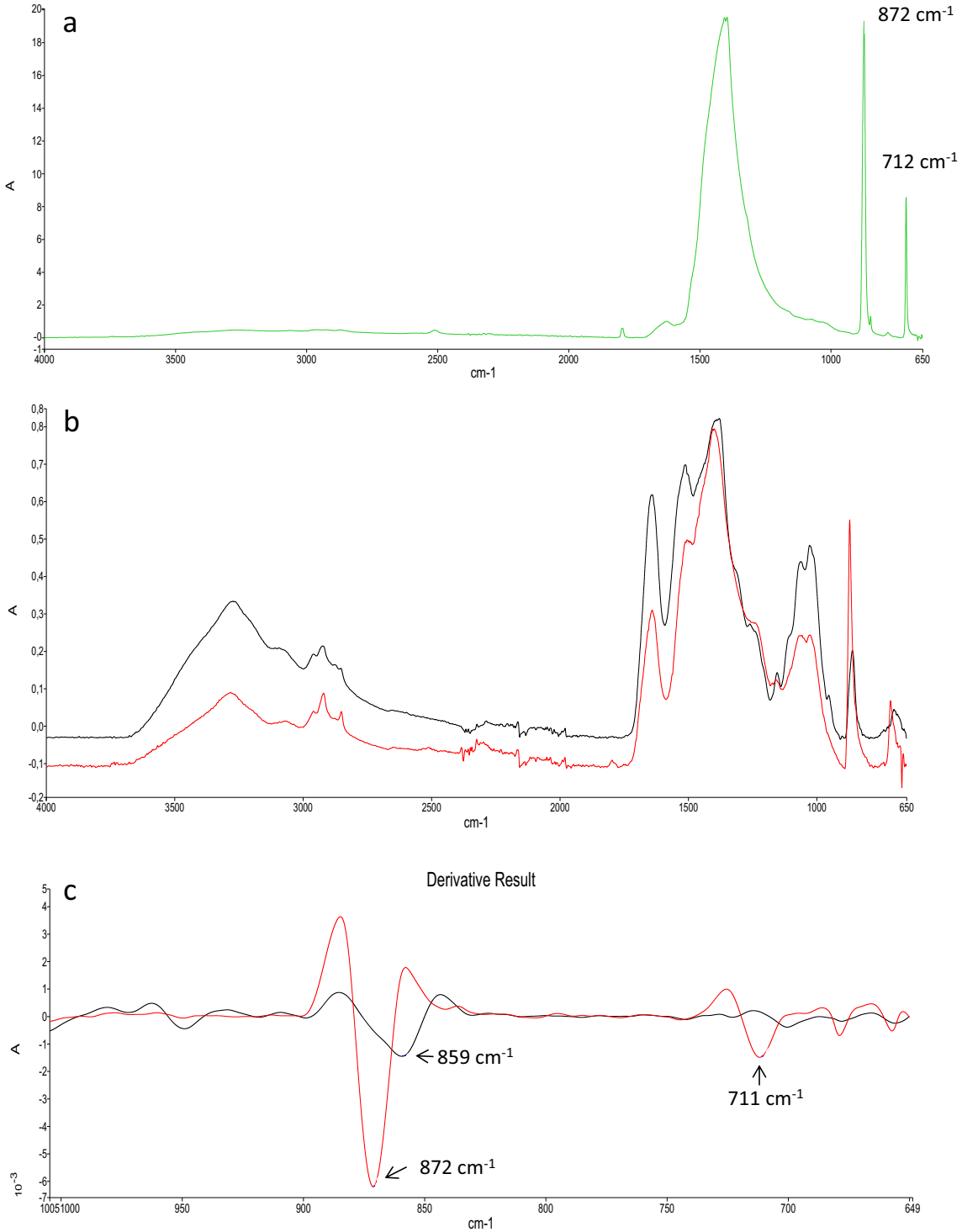

Fig. 2 Representative ATR–FTIR spectrum of (**a**) Calcium carbonate, (**b**) powdered crayfish cephalothorax (*Astacus leptodactylus*) incubated with lead (0.01 ppm) (red line) and without lead (black line). The arrow indicates the shifted peak. Incubation with cadmium, chromium, lead, nickel, and zinc, at all tested concentrations (0.01, 0.1, 1.0, 10.0 ppm), gave similar results. Second derivative (**c**) where the shift from 859 to 872 cm^{-1} is evidenced along with the appearance of the peak at 712 cm^{-1}

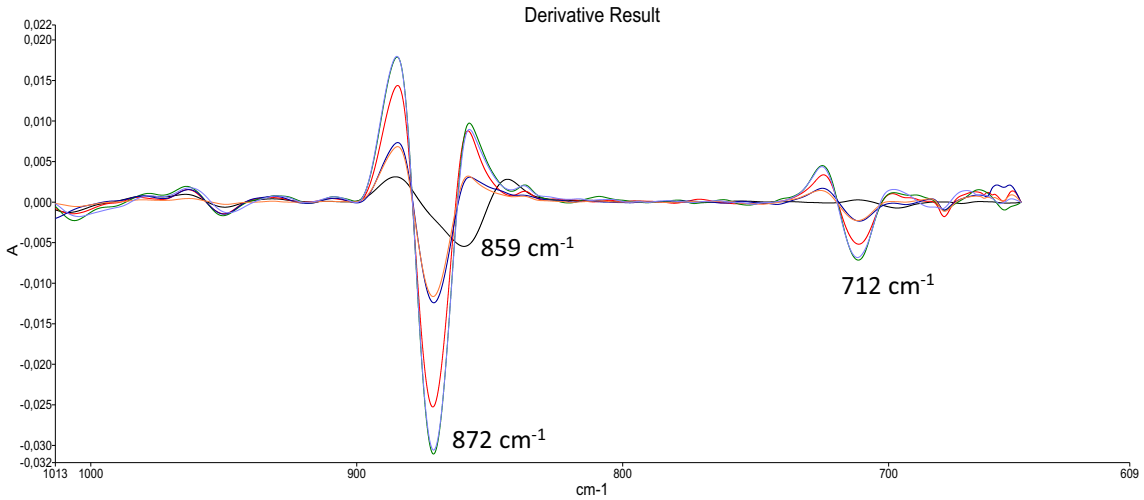

Fig. 3 Second derivative showing the shift from 859 to 872 cm^{-1} and the appearance of the peak at 712 cm^{-1}, after incubation of *Astacus leptodactylus* cephalothorax (black line) with cadmium (green line), chromium (orange line), lead (red line), nickel (blue line), and zinc (light blue line)

the positive HM ions that move the calcium ion, forming coordination bonds with the carbonate ion. Many adducts are classified as coordination compounds since their chemistry is easily described considering a central Mn + atom or ion around which a large variety of molecules or ions called ligands can be arranged. The charge of the resulting complex is determined by the metal charge and the sum of the binder charges. In fact, the forming complex is a chemical compound in which an atom binds a number of other chemical species higher than its oxidation number (Escuer et al. 1997; Erras-Hanauer et al. 2003; Casas et al. 2006). We hypothesize that the coordination bonds between HM and the carbonate ion induce a sort of crystalline organization visible in the spectrum at 712 cm^{-1}. Consequently, the out-of-plane bending shifts to 872 cm^{-1} can be attributable to the different chemical environment that is created as a consequence of the links established between HM and the carbonate ion.

In the ATR–FTIR spectrum of the cephalothorax exoskeleton incubated with HM, the absorbance of the broad peak comprised between 1200 and 1600 cm^{-1} and the peak in the range 1050–950 cm^{-1} increase, although not linearly with the HM concentration, likely the consequence of the HM binding to the protein and chitin components (Luquet et al. 2013).

Recently, the ACC properties of binding the HM have gained a great deal of attention. Freshwater bodies contaminated by HM and other toxic substances have become a worldwide emergency calling for remediation strategies. The use of ACC as a HM binder can be regarded as an economically sound strategy to remove HM and other toxic substances from the environment (Cai et al. 2010). Cluster separation, found by a PCA analysis using the SIMCA algorithm, was obtained in those wavelength ranges corresponding to 900–650 cm^{-1} indicating a good separation between groups. According to the SIMCA models, the larger interclass distance among groups, the better separation. It is generally accepted that the distance value higher than 3 is indicative that the samples are well separated and hence different (He et al. 2007).

It is well known that calcium carbonate is the main sorbent for a variety of metals in carbonate aquifers (Zachara et al. 1991). In a study carried out by Aziz et al. (2008), the binding of HM (Cd, Pb, Zn, Ni, Cu, and Cr) to limestone was influenced by the media surface but not by the pH, indicating that the HM removal is a chemical phenomenon. Moreover, HM binding to calcium carbonate has been shown to be influenced by the $CaCO_3$ surface; thus, we analyzed the FTIR profile of crayfish cephalothorax exoskeleton as a whole incubated with HM up to 4 weeks. The FTIR profile of the cephalothorax exoskeleton in the form of powder was similar to the FTIR profile of the cephalothorax exoskeleton as a whole. Changes in the FTIR profile have been visible since the first week of incubation. The out-of-plane bending peak at 859 cm^{-1}, typical of ACC, shifted to 872 cm^{-1} and both the in-plane bending of carbonate peak at 712 cm^{-1} and the out-of-plane bending peak at 872 cm^{-1} increased during the incubation time, proportionally with the HM

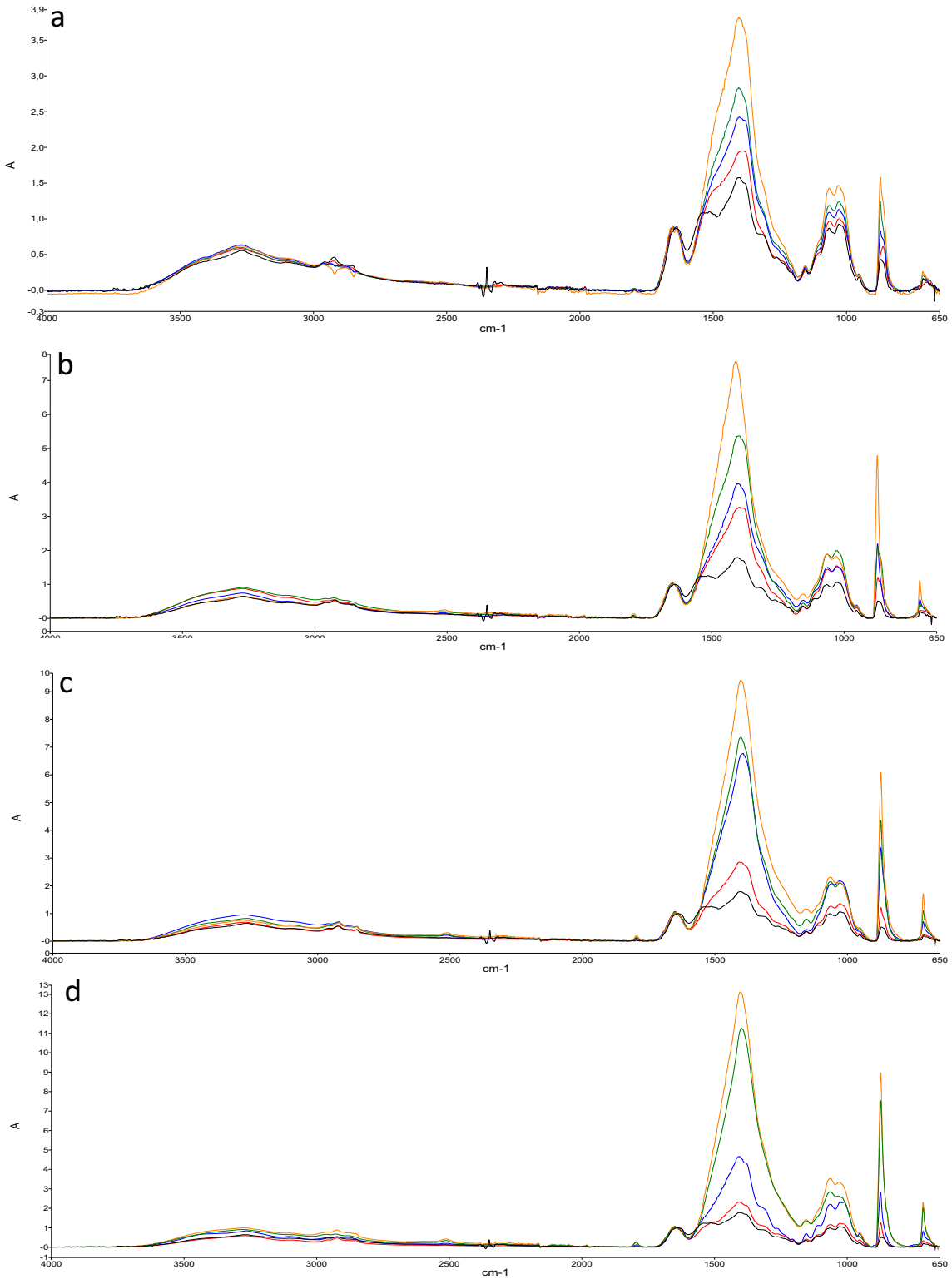

Fig. 4 *Astacus leptodactylus* cephalothorax incubated with lead at 1 week (**a**), 2 weeks (**b**), 3 weeks (**c**), and 4 weeks (**d**) showed the increase in the absorbance of the peaks in the ranges 1560–1350 cm^{-1} and 1070–990 cm^{-1}. Red line, lead 0.01 ppm; blue line, lead 0.1 ppm; green line, lead 1.0 ppm; orange line, lead 10.0 ppm; black line, cephalothorax

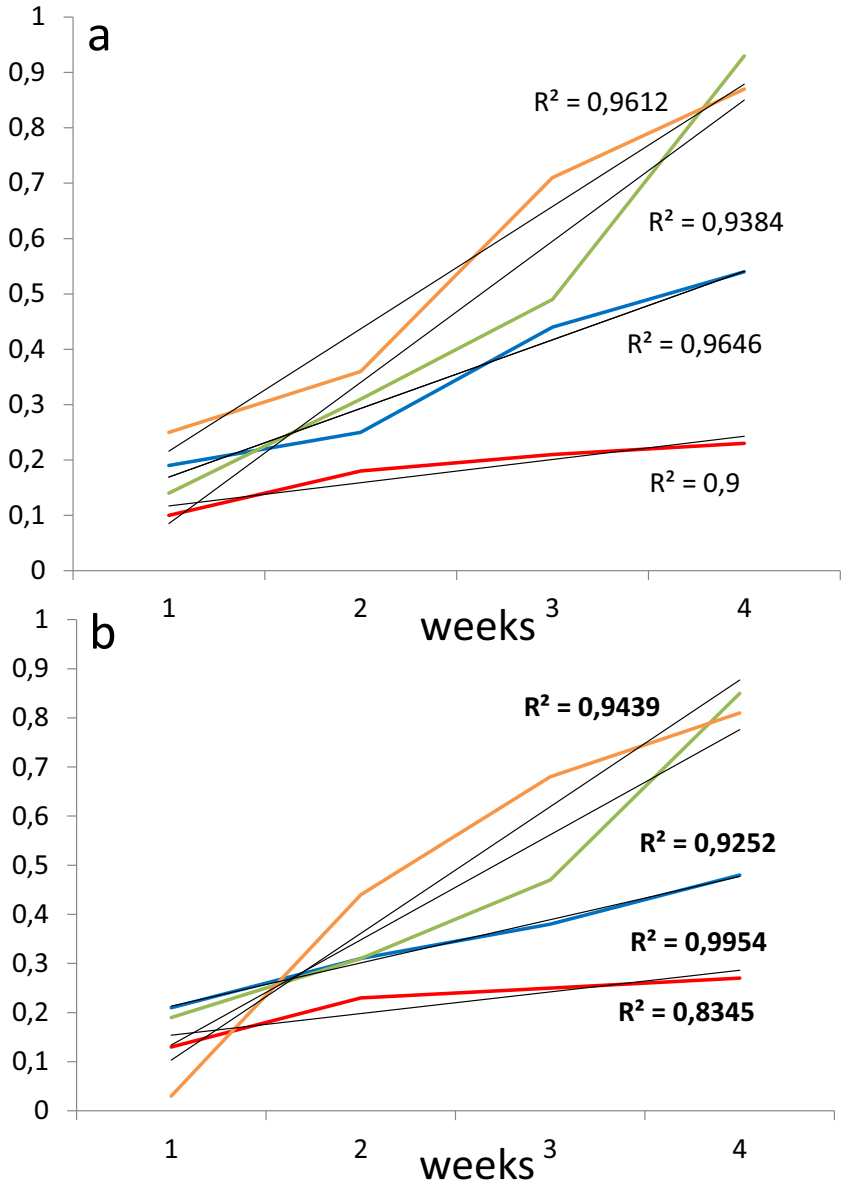

Fig. 5 Correlation between the area of the peak 872 cm^{-1} (**a**) and 712 cm^{-1} (**b**) and the lead concentration during 4 weeks of incubation with the whole crayfish cephalothorax (*Astacus leptodactylus*). Red line, 0.01 ppm; blue line, 0.1 ppm; green line, 1.0 ppm; orange line, 10.0 ppm; black line, tendency line. The concentrations 0.1 and 10.0 ppm gave similar results. Incubation with cadmium, chromium, nickel, and zinc, at all tested concentrations (0.01, 0.01, 1.0, 10.0 ppm), gave similar results

concentration from 0.01 to 10.0 ppm. This study showed that the HM binding to the cephalothorax exoskeleton was both dose and time-dependent. In this study, the increase in 872 and 712 cm^{-1} peaks absorbance was indeed linear during the 4 weeks of incubation with the time and the concentration of the HM.

After 4 weeks of clearance, the FTIR profile showed the typical peak shift to 872 cm^{-1} and the peak at 712 cm^{-1}. The peaks in correspondence to proteins and chitin appeared less broad after 4 weeks of clearance, although there was not a correlation between the peak area and the clearance time for any concentration of HM used. All together, the FTIR profile points at the presence of HM binding to the cephalothorax exoskeleton, indicating a quite stable binding.

Conclusions

In conclusions, the incubation of the cephalothorax exoskeleton with Cd, Cr, Pb, Ni, and Zn revealed qualitative ATR–FTIR profile modifications: the shift of the peak from 859 to 872 cm^{-1} and the appearance of a peak at 712 cm^{-1}. Both modifications are ascribable to the HM interaction with the calcium carbonate component of the cephalothorax

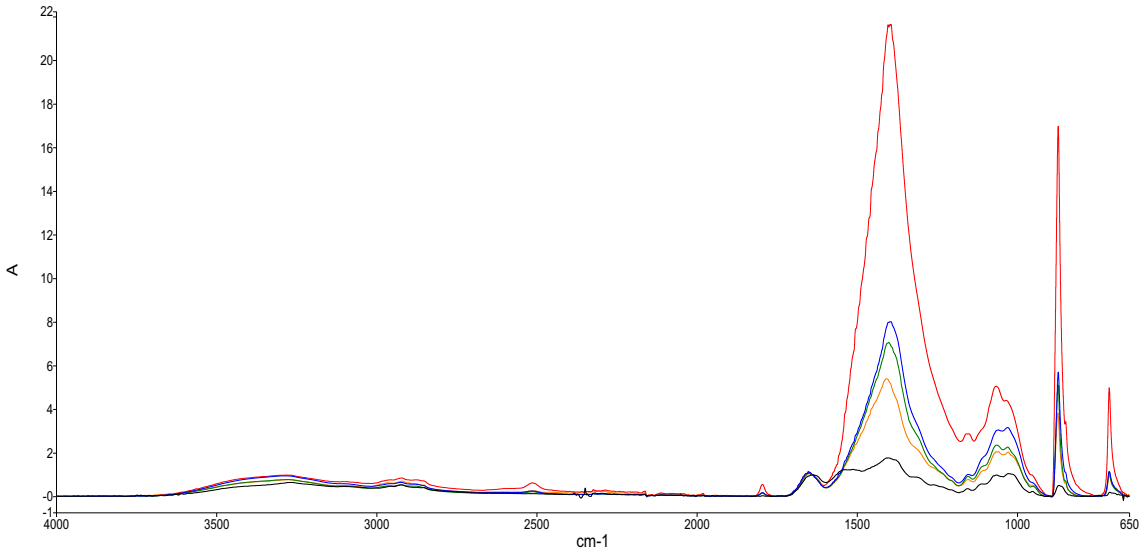

Fig. 6 Representative ATR–FTIR spectrum of the clearance of the whole crayfish cephalothorax (*Astacus leptodactylus*) incubated with fresh water for 4 weeks, after 4 weeks of incubation with lead (1.0 ppm). Red line, first week of clearance; blue line, second week of clearance; green line, third week of clearance; orange line, fourth week of clearance; black line, control. The concentrations 0.01, 0.1, and 10.0 ppm gave similar results. Incubation with cadmium, chromium, nickel, and zinc, at all tested concentrations (0.01, 0.1, 1.0, 10.0 ppm), gave similar results

exoskeleton. The absorbance of the peaks increased along with the time of incubation and the HM concentration. We conclude that ATR–FTIR analysis of crayfish cephalothorax exoskeleton is a useful, quick, and cost sensitive tool to detect HM presence in the environment. Only the transition metals, which by their nature form coordination bonds with carbonate, produce a shift in frequencies when subjected to ATR–FTIR analysis; however, it has to be regarded as a non-specific analytical technique for assessing HE contamination, since unable to discriminate between different HM.

References

Addadi L, Raz S, Weiner S (2003) Taking advantage of disorder: amorphous calcium carbonate and its role in biomineralization. Adv Mater 15(12):959–970

Alcorlo P, Otero M, Crehuet M, Baltanás A, Montes C (2006) The use of the red swamp crayfish (*Procambarus clarkii*, Girard) as indicator of the bioavailability of heavy metals in environmental monitoring in the River Guadiamar (SW, Spain). Sci Total Environ 366:380–390

Ali H, Khan E, Ilahi I (2019) Environmental chemistry and ecotoxicology of hazardous heavy metals: environmental persistence, toxicity, and bioaccumulation. J Chemother:6730305. https://doi.org/10.1155/2019/6730305

Alikhan MA, Bagatto G, Zia S (1990) The crayfish as a "biological indicator" of aquatic contamination by heavy metals. Water Res 24:1069–1076

Andersen FA, Brecevic L (1991) Infrared spectra of amorphous and crystalline calcium carbonate. Acta Chem Scand 45:1018–1024

Anderson RV, Brower JE (1978) Patterns of trace metal accumulation in crayfish populations. 2 Dept. of Biological Sciences, Northem Illinois University, Dekalb, III. Bull Environ Contam Toxicol 20: 120–127

Assi MA, Hezmee MNM, Haron AW, Sabri MYM, Rajion MA (2016) The detrimental effects of lead on human and animal health. Vet World 9:660–671

Aziz HA, Adlan MN, Ariffin KS (2008) Heavy metals (Cd, Pb, Zn, Ni, Cu and Cr (III)) removal from water in Malaysia: post treatment by high quality limestone. Bioresour Technol 99:1578–1583

Bruno G, Volpe MG, De Luise G, Paolucci M (2006) Detection of heavy metals in farmed Cherax destructor. Bull Fr Pêche Piscic 380-381: 1341–1349

Cai G-B, Zhao G-X, Wang X-K, Yu S-H (2010) Synthesis of polyacrylic acid stabilized amorphous calcium carbonate nanoparticles and their application for removal of toxic heavy metal ions in water. J Phys Chem C 114:12948–12954

Casas JS, Sordo J, Vidarte MJ (2006) Chapter 2 - Lead(II) coordination chemistry in the solid state Lead. In: JS Casas, J Sordo (eds) Lead 1st Edition, Chemistry, Analytical Aspects, Environmental Impact and Health Effects. Elsevier, Amsterdam, pp 41–99

Del Ramo J, Díaz-Mayans J, Torreblanca A, Núñez A (1987) Effects of temperature on the acute toxicity of heavy metals (Cr, Cd and Hg) to the freshwater crayfish, *Procambarus clarkii* (Girard). Bull Environ Contam Toxicol 38:736–741

Erras-Hanauer H, Mao Z-W, Liehr G, Clark T, van Eldik R (2003) Structures of carbonato and bicarbonato complexes of Bis (1,10-phenanthroline) zinc(II): experiment and theory. Eur Inorg Chem 8:1562–1569

Escuer A, Vicente R, Kumar SB, Solans X, Font-Bardía M (1997) A novel tridentate co-ordination mode for the carbonato nickel system. J Chem Soc Dalton Trans 3:403–407

Giraud-Guille MM, Belamie E, Mosser G (2004) Organic and mineral networks in carapaces, bones and biomimetic materials. Comptes Rendus Palevol 3:503–513

Goretti E, Pallottini M, Ricciarini MI, Selvaggi R, Cappelletti D (2016) Heavy metals bioaccumulation in selected tissues of red swamp crayfish: an easy tool for monitoring environmental contamination levels. Sci Total Environ 559:339–346

He J, Rodriguez-Saona LE, Giusti MM (2007) Mid infrared spectroscopy for juice authentications rapid differentiation of commercial juices. J Agric Food Chem 55:4443–4452

Huner JV, Kononen H, Lindquist O (1990) Variation in body composition and exoskeleton mineralization as functions of the molt and reproductive cycles of the noble crayfish, *Astacus astacus* L. (decapoda, astacidae), from a pond in central Finland. Comp Biochem Physiol 96A:235–240

Iconomidou VA, Chryssikos GD, Gionis V, Willis JH, Hamodrakas SJ (2001) Soft-cuticle protein secondary structure as revealed by FT-Raman, ATR-FTIR and CD spectroscopy. Insect Biochem Mol Biol 31:877–885

Igiri BE, Okoduwa SIR, Idoko GO, Akabuogu EP, Adeyi AO, Ejiogu IK (2018) Toxicity and bioremediation of heavy metals contaminated ecosystem from tannery wastewater: a review. J Toxicol:2568038. https://doi.org/10.1155/2018/2568038

Jaishankar M, Tseten T, Anbalagan N, Mathew BB, Beeregowda KN (2014) Toxicity, mechanism and health effects of some heavy metals. Interdiscip Toxicol 7:60–72

Jussila J (1997) Carapace mineralization and hepatopancreatic indices in natural and cultured populations of marron (*Cherax tenuimanus*) in Western Australia. Mar Freshw Res 48:67–72

Jussila J, Henttonen P, Huner JV (1995) Calcium, magnesium and manganese content of noble crayfish (*Astacus astacus* L) brancial carapace and its relationship to water and sediment mineral contents of two ponds and one lake in Central Finland. Freshwater Crayfish 10: 230–238

Kouba A, Buřič M, Kozák P (2010) Bioaccumulation and effects of heavy metals in crayfish:a review. Water Air Soil Pollut 211:5–16

Kuklina I, Kouba A, Kozák P (2013) Real-time monitoring of water quality using fish and crayfish as bio-indicators: a review. Environ Monit Assess 185:5043–5053

Kuklina I, Kouba A, Buli M, Horká I, Duriš Z, Kozák P (2014) Accumulation of heavy metals in crayfish and fish from selected Czech reservoirs. Hindawi Publishing Corporation. Biomed Res Int:306103. https://doi.org/10.1155/2014/306103

Luquet G, Fernández MS, Badou A, Guichard N (2013) Comparative ultrastructure and carbohydrate composition of gastroliths from astacidae, cambaridae and parastacidae freshwater crayfish (Crustacea, Decapoda). Biomolecules 3:18–38

Morel FMM, Hering JG (1993) Principles and applications of aquatic chemistry. Wiley-Interscience, New York

Movasaghi Z, Rehman S, Rehman IU (2008) Fourier transform infrared (FTIR) spectroscopy of biological tissues. Appl Spectrosc Rev 43: 134–179

Pallottini M, Goretti E, Gaino E, Selvaggi R, Cappelletti D, Céréghino R (2015) Invertebrate diversity in relation to chemical pollution in an Umbrian stream system (Italy). C R Biol 338:511–520

Prashanth L, Kattapagari KK, Chitturi RT, Baddam VRR, Prasad LK (2015) A review on role of essential trace elements in health and disease. J Dr NTR Univ Health Sci 4:75–85

Rajaganapathy V, Xavier F, Sreekumar D, Mandal PK (2011) Heavy metal contamination in soil, water and fodder and their presence in livestock and products: a review. Int J Environ Sci Technol 4:234–249

Shechter A, Berman A, Singer A, Freiman A, Grinstein M, Erez J, Aflalo EH, Sagi A (2008) Reciprocal changes in calcification of the gastrolith and cuticle during the molt cycle of the red claw crayfish *Cherax quadricarinatus*. Biol Bull 214:122–134

Simonescu CM (2012) Application of FTIR spectroscopy in environmental studies. InTech Open. https://doi.org/10.5772/48331

Stein RA, Murphy ML (1976) Changes in proximate composition of the crayfish *Orconectes propinquus* with size, sex, and life stage. J Fish Res Board Can 33:2450–2458

Suárez–Serrano A, Alcaraz C, Ibáñez C, Trobajo R, Barata C (2010) *Procambarus clarkii* as a bioindicators of heavy metal pollution sources in the lower Ebro River and Delta. Ecotoxicol Environ Saf 73:280–286

Sugawara A, Nishimura T, Yamamoto Y, Inoue H, Nagasawa H, Kato T (2006) Self-organization of oriented calcium carbonate/polymer composites: effects of a matrix peptide isolated from the exoskeleton of a crayfish. Angew Chem Int Ed 45:2876–2879

Tao J (2013) FTIR and Raman studies of structure and bonding in mineral and organic-mineral composites. Methods Enzymol 532:533–556

Volpe G, Monetta M, Di Stasio M, Paolucci M (2008) Rheological behavior of polysaccharide based pellets for crayfish feeding tested on growth in the crayfish *Cherax albidus*. Aquaculture 274:339–346

Volpe MG, Varricchio E, Coccia E, Santagata G, Di Stasio M, Malinconico M, Paolucci M (2012) Manufacturing pellets with different binders: effect on water stability and feeding response in juvenile *Cherax albidus*. Aquaculture 324-325:104–110

Volpe MG, Coccia E, Parrillo L, Paolucci M (2018) Evaluation of metabolic changes induced by polyphenols in the crayfish *Astacus leptodactylus* by metabolomics using Fourier transformed infrared spectroscopy. J Biosci 43:585–596

Volpe MG, Coccia E, Siano F, Di Stasio M, Paolucci M (2019) Rapid evaluation methods for quality of trout (*Oncorhynchus mykiss*) fresh fillet preserved in an active edible coating. Foods 8:113. https://doi.org/10.3390/foods8040113

Wang Y, Wang S, Sun H, Lei J, Ye T, Lin L, Wang L (2016) Crayfish carapace powder adsorbing heavy metal ions from aqueous solution: capacity, characterization, mechanism. J Aquat Food Prod Technol 25:122–130

Zachara JM, Cowan CE, Resch CT (1991) Sorption of divalent metals on calcite. Geochim Cosmochim Acta 55:1549–1562

Zheng X, Li B, Zhu B, Kuang R, KuangX XB, Ma M (2010) Crayfish carapace micro-powder (CCM): a novel and efficient adsorbent for heavy metal ion removal from wastewater. Water 2:257–272

Zhou Q, Zhang J, Fu J, Shi J, Jiang G (2008) Biomonitoring: an appealing tool for assessment of metal pollution in the aquatic ecosystem. Anal Chim Acta 606:135–150